New features of electron diffusion regions observed at subsolar magnetic field reconnection sites

F. S. Mozer,[1] S. D. Bale,[1] J. P. McFadden,[1] and R. B. Torbert[2]

Received 15 July 2005; revised 11 October 2005; accepted 9 November 2005; published 17 December 2005.

[1] Nineteen electron diffusion regions at magnetic field reconnection sites have been found in one hour of Cluster satellite data near the subsolar magnetopause. Investigations on previously unachieved spatial and temporal scales show the following for the first time: direct conversion of magnetic energy to electron energy (The resulting accelerated electrons, their field-aligned currents, and their post-acceleration fate were measured); the spatial dimensions of the large electric fields in the electron diffusion regions have an average thickness of 0.3 times the electron skin depth, in agreement with theory; and these electron diffusion regions were topological boundaries between open and closed magnetic field geometries that contained different plasma and magnetic field line flows. The electron diffusion regions were located at the magnetospheric separatrix where the magnetic field was large and the electron beta was less than one. **Citation:** Mozer, F. S., S. D. Bale, J. P. McFadden, and R. B. Torbert (2005), New features of electron diffusion regions observed at subsolar magnetic field reconnection sites, *Geophys. Res. Lett.*, *32*, L24102, doi:10.1029/2005GL024092.

[2] Magnetic field reconnection converts magnetic energy to particle energy on time scales much shorter than magnetic field diffusion times. For this reason, reconnection is important to plasma dynamics and particle acceleration in the laboratory, the terrestrial magnetosphere and astrophysics. The key region of reconnection is the electron diffusion region, the site of previously unobserved electron demagnetization, electromagnetic energy conversion to accelerated electrons, and the connection of magnetic fields coming from different topologies. Electron diffusion regions with these properties have been found in the Cluster satellite data at the subsolar magnetopause by searching for regions having [*Mozer*, 2005]:

[3] - A non-zero parallel electric field (because such a field is required for magnetic field lines to reconnect) [*Longmire*, 1963]

[4] - A structure whose scale size is $\sim c/\omega_{pe} \sim 4$ km [*Vasyliunas*, 1975]

[5] - A perpendicular electric field that is much larger than the typical reconnection tangential electric field of $\sim$0.5 mV/m (in order that diffusion be effective).

[6] - A large conversion of electromagnetic energy, $\mathbf{j}\cdot\mathbf{E} \gg 0$

[7] - The acceleration of electron beams

[8] - A change of the magnetic field topology and the $\mathbf{EXB}/B^2$ flow across the boundary.

No limitations on the magnetic field strength or the electron beta are imposed on the search for electron diffusion regions. An operational definition of the term "electron diffusion region" used in this paper is any region that satisfies the above criteria.

[9] The three-axis electric field experiment on Polar observed hundreds of electron diffusion regions whose parallel electric field magnitudes averaged 30% of the average 38 mV/m perpendicular electric field [*Mozer et al.*, 2003; *Mozer*, 2005]. These fields were found in filamentary current structures whose scale sizes were $\sim c/\omega_{pe}$, but the time resolution of the measurement was not adequate for more accurate estimates. These electron diffusion regions were found both inside the reconnection layer and at its magnetospheric separatrix where, in both cases, the electron beta was generally less than one. Of the $\sim$400 orbits searched in three years of Polar data, 70 of 117 events occurred during 12 orbits. Thus, the majority of magnetopause crossings did not yield verified electron diffusion regions.

[10] In this paper, data from 1415 to 1515 UT on January 25, 2005 from the four Cluster spacecraft are analyzed to demonstrate the existence of 19 electron diffusion regions that were all located at the magnetospheric separatrix. The thicknesses of these regions were measured quantitatively, the direct observation of electron beams accelerated in the electron diffusion region is demonstrated, and the topological changes of $\mathbf{EXB}/B^2$ and the plasma properties across an electron diffusion region are shown. The four Cluster spacecraft are not directly able to measure the parallel electric field. However, the parallel electric field events on Polar allow the inference that the structures observed by Cluster are electron diffusion regions that satisfy the above criteria.

[11] Figure 1 presents four minutes of data from Cluster spacecraft 2 at a geocentric altitude of 12 earth radii, latitude of 28 degrees, and magnetic local time of 1510. Figure 1a gives the plasma density inferred from the spacecraft potential, and Figure 1b gives the electron energy flux integrated over solid angle as measured by the PEACE instrument. The low density regions of Figure 1a, having a relative dearth of low energy electrons in Figure 1b, are identified as the magnetosphere while the higher density and more intense low energy electron regions signify the near-earth magnetopause. Figure 1c gives one component of the raw electric field [*Gustafsson et al.*, 1997] measured every 2.2 milliseconds, while Figures 1d and 1e give the fluxes of 500 eV electrons moving parallel and anti-parallel to the magnetic field, as measured with an eight millisecond time resolution by the Electron Drift Instrument

[1]Space Sciences Laboratory, University of California, Berkeley, California, USA.
[2]Physics Department and Space Science Center, University of New Hampshire, Durham, New Hampshire, USA.

0094-8276/05/2005GL024092$05.00

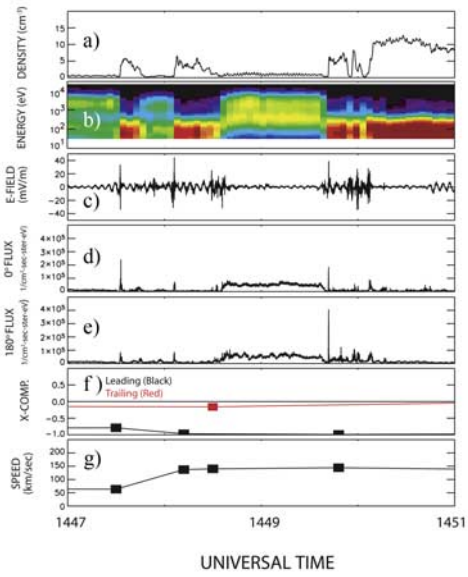

Figure 1. Plasma and field parameters measured on Cluster spacecraft 2 during a four minute interval.

[*Paschmann et al.*, 1997]. The narrow peaks in the electric field and the field aligned electron fluxes indicate electron diffusion regions at the boundaries of the magnetospheric and magnetosheath plasmas. Such peaks appear at the five abrupt density increases in Figure 1a and, to a lesser extent, at some of the four slower decreases back to the magnetospheric plasma density.

[12] The electron diffusion regions in Figure 1 and during the hour of interest were found at the magnetospheric side of the reconnection layer where the density was $\sim$1 cm^{-3}, B_Z was $\sim$25 nT, and the electron beta was <0.1. Thus, electron diffusion regions are not found just at nulls in the reconnection magnetic field or where the plasma beta is large, as is sometimes assumed.

[13] Because the $\sim$1 keV magnetospheric electrons in Figure 1b disappeared and the cold magnetosheath electrons appeared at each entry into the magnetosheath, the spacecraft must have moved from closed to open magnetic field lines, which shows that the electron diffusion regions separated regions of different topologies. The magnetic field directions were within seven degrees of the plane of these electron diffusion regions. These facts are consistent with the electron diffusion regions being separatricies on the magnetospheric side of the reconnection layer.

[14] Figure 2 presents 11 seconds of data during the crossing of an electron diffusion region over the four Cluster spacecraft. Figures 2a–2h give plots for each spacecraft of plasma density and electric field, organized vertically from spacecraft 1 in Figures 2a and 2b to spacecraft 4 in Figures 2g–2h. For each spacecraft, large electric fields ($\leq$ 100 mV/m) were observed at the foot of the density increase. Relative to spacecraft 1, the spacecraft separations were 1255 to 1432 kilometers and the time differences in the observations of the electric field spikes were −3.38 to +5.53 seconds. From this data and the assumption of a planar boundary moving along its normal at a constant velocity, a boundary speed of 137 km/sec and a boundary normal in GSE coordinates of (−0.974, 0.029, −0.224) are determined. From the average plasma density at these crossings, the electron skin depth was 4.7 km. These data show that the electron diffusion region had a spatial scale of at least 1400 km in the plane ($\sim$300 electron skin depths), and a temporal stability of at least 9 seconds. Thus, these electron diffusion regions are thin in one dimension, extensive in the two other dimensions, and they exist for thousands of plasma periods.

[15] The GSE x-component of each boundary normal and the boundary speeds at four of the 19 electron diffusion region passages during the hour of interest are given in Figures 1f and 1g. (These points do not exactly line up with the spikes in the electric field and the field aligned electron fluxes because they are plotted at the average time of the crossings over the four spacecraft and not the time associated with passage over spacecraft 2. There are fewer points in Figures 1f and 1g than there are peaks in the electric field and field aligned fluxes because not all spacecraft observed all crossings and data from four spacecraft are required to produce this data.) The leading edges of density enhancements had the more well-defined large electric fields and they moved in the anti-sunward direction. These leading edge motions and the trailing edge motions, primarily in the GSE Y-direction, are consistent with bulges on the magnetopause that moved tailward across the spacecraft without the spacecraft penetrating into the magnetosheath proper. These structures have many of the characteristics associated with flux transfer events [*Russell and Elphic*, 1979].

[16] Because the magnitude of the main magnetic field changed little during the electron diffusion region events while its components varied, these crossings must have been associated with field-aligned currents. These currents were directly observed as the difference between the 0 and 180 degree electron fluxes measured by EDI. Figure 3 presents 1.2 seconds of data that provide one example of this flux difference and the rotation of a magnetic field

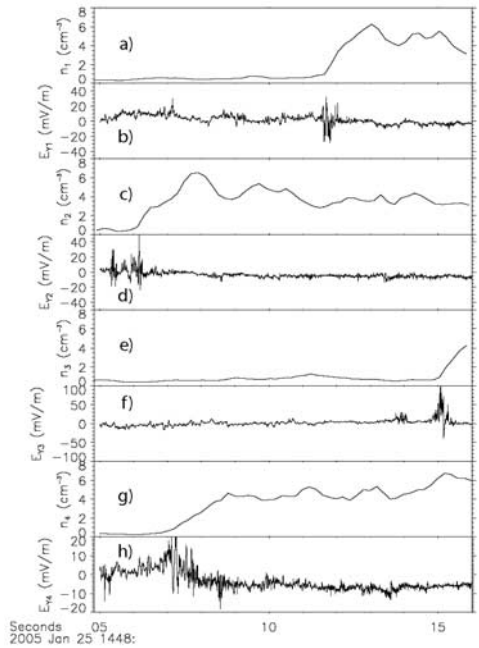

Figure 2. Plasma density and one component of the electric field measured on the four Cluster spacecraft as an electron diffusion region passed over them.

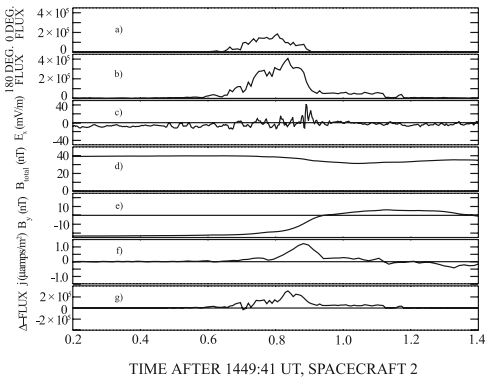

Figure 3. Magnetic field variation and field-aligned current obtained from plasma measurements on Cluster spacecraft 2.

component associated with it. Figures 3a and 3b give the 0 and 180 degree electron fluxes measured by EDI, while Figure 3c gives one component of the electric field. Figures 3d and 3e provide the total magnetic field and its y-component. Because the magnetic field was largely in the z-direction while the boundary motion was in the negative x-direction, a field aligned current sheet would produce the rotation of B_Y that is observed in Figure 3e. The current density obtained from the variation of B_Y is plotted in Figure 3f. The difference between the 0 and 180 degree electron fluxes is plotted for comparison in Figure 3g. The form of the data in the two panels is quite similar except for a 30 millisecond time offset that may be instrumental. A quantitative agreement between the amplitudes of the Figures 3f and 3g data cannot be determined because neither the electron angular distribution nor its energy spectrum is known with sufficient temporal resolution from the PEACE data. However, assuming typical values of these parameters, there is a better than qualitative agreement between the two panels.

[17] The parallel current density of Figure 3 may be combined with an estimate of the parallel electric field and the known plasma density to produce an estimate of the parallel electromagnetic energy conversion per particle per second ($j_{||}E_{||}/n$). In 117 events observed on Polar, the average parallel electric field was 30% of the perpendicular field [*Mozer*, 2005]. From this, the estimated parallel electric field is 12 mV/m. The parallel current was $\sim 1.5 \times 10^{-6}$ amps/m^2 and the density was 4 particles/cm^3. The combination of these values gives an electromagnetic energy conversion per particle per second of $\sim$30 keV. Because a typical electron resides in the electron diffusion region for several milliseconds, it acquires a typical energy of a few hundred eV. Thus, the electrons accelerated by this electromagnetic energy conversion produced the observed parallel and anti-parallel electron fluxes and the net field-aligned current. They are also probably the source of the $\sim$100 eV counter-streaming magnetospheric electrons observed by the PEACE instrument and seen as the integrated flux in Figure 1b after each electron diffusion region encounter.

[18] An expanded plot of the passage of the electron diffusion region of Figure 2 over spacecraft 3 is given in the 0.7 second plots of Figure 4. As the density of Figure 4a increased from less than 1 to about 4 cm^{-3}, there were electric field pulses as large as 100 mV/m (Figure 4b), 500 eV electron beams parallel and anti-parallel to the magnetic field (Figure 4c), and steps in the magnetic field (Figure 4e). If these magnetic field steps were due to spatial variations they would indicate that the current was filamentary, while, if they were temporal, they would be associated with the curl of the observed electric field spikes. On the finest time scale, these impulsive events are not aligned. If the misalignment was not instrumental, they may be signals of time dependent phenomena such as sloshing electron beams in the presence of large electric fields. Because the maximum of $(\varepsilon_o/2)E^2/nkT$ was an order-of-magnitude larger than the electron-to-ion mass ratio, non-linear physics inside the electron diffusion region may be important.

[19] It is noted in Figure 4 as well as in the earlier Polar electron diffusion region data [*Mozer et al.*, 2003] that fluctuations of density comparable to the average density occur within the electron diffusion region. If these are spatial and not temporal variations, the effective electric field associated with the divergence of the pressure tensor in the Generalized Ohm's Law is sufficient to account for the non-zero parallel electric field and the microphysics of the electron beam acceleration.

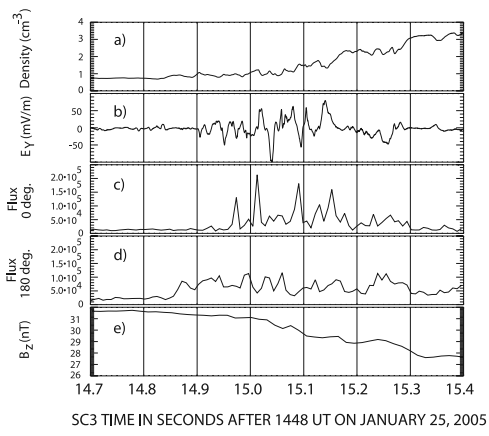

Figure 4. Expanded view of the passage of the electron diffusion region of Figure 2 over spacecraft 3.

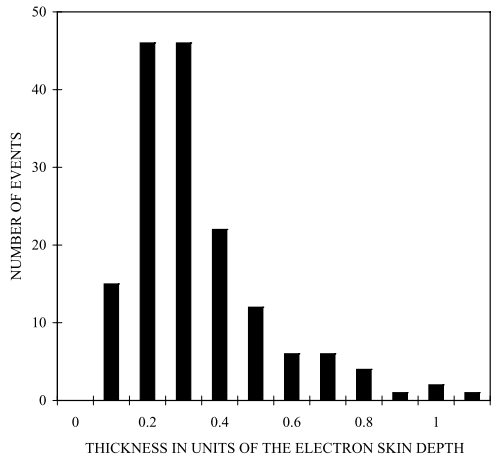

Figure 5. Histogram of the full-widths-at-half-maxima of the electric field pulses observed during one hour of data from four spacecraft. The individual widths are normalized to the electron skin depth.

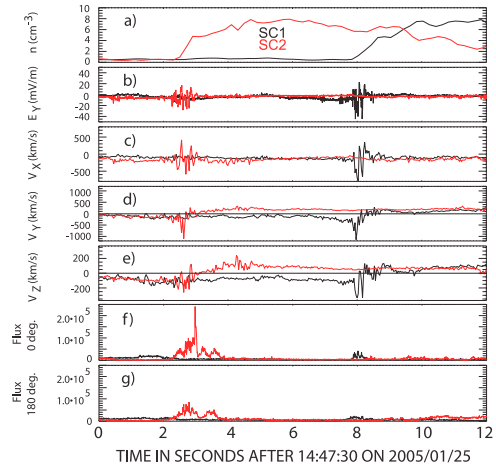

Figure 6. Passage of an electron diffusion region over two spacecraft.

[20] A histogram of the full widths at half maximum of the large, impulsive electric fields in the electron diffusion regions is given in Figure 5. The average pulse width for all crossings was 0.3 c/ω_{pe} while, for the high speed crossings, it was 0.4 c/ω_{pe}. These are estimates of the average width of a single electric field spike and, because several such spikes existed within a single region, the total thickness of a full structure was a few electron skin depths. These electric field spikes occur predominantly in the perpendicular component because this is the larger component. That the widths of the non-measured parallel component may be larger is suggested by theory [*Bhattacharjee et al.*, 2005]. It is also noted that the field aligned electron flux spikes have a width that is similar to the electric field spikes.

[21] In the standard picture of reconnection, the electron diffusion region is a boundary across which the tangential **EXB**/B^2 flow changes because the fields on the two sides are decoupled. A similar topological change across the electron diffusion regions occurred on Cluster as is illustrated by the 12 seconds of data in Figure 6. During this interval, an electron diffusion region crossed spacecraft 2 (red data curves) about five seconds before it crossed spacecraft 1 (black data curves). At the crossing over either of the spacecraft, the plasma density of Figure 6a increased; there were large impulsive electric fields in Figure 6b; the three GSE-components of the 15 Hz low-pass-filtered **EXB**/B^2 flow of Figures 6c–6e exhibited turbulent flows as large as 1000 km/sec; and the counter-streaming electron fluxes of Figures 6f and 6g increased. (It is noted that the field-aligned fluxes and currents of Figures 6f and 6g differed by an order-of-magnitude at the two crossings, due either to temporal or spatial effects.) During the initial or final two seconds of the plot, while the two spacecraft were on the same side of the electron diffusion region, the components of **EXB**/B^2 in Figures 6c–6e were the same on the two spacecraft. However, in the central third of the plot, while the two spacecraft were on opposite sides of the boundary, the tangential y and z components of the flow were in opposite directions at the two spacecraft. This topological difference was constant for a period of at least several seconds.

[22] The properties of the observed electron diffusion regions in the one hour of Cluster data are consistent with those attributed to separatrices on the magnetospheric side of the reconnection layer. Namely, they extend over large distances; a long dimension is nearly parallel to the local magnetic field; they contain field aligned electron beams and electric fields; there is a topological change in the **EXB**/B^2 flow across them; the magnetic field geometry changes from closed to open across them; and their thickness is the order of the electron skin depth. These features have been observed in simulations [*Shay et al.*, 2001] and earlier reported Polar data [*Mozer et al.*, 2002, Figure 4].

[23] **Acknowledgments.** This work was performed under NASA Grants NAG5-11733, NAG5-11944, and NNG04GA46G. The authors thank A. Fazakerley, E. Georgescu, and M. Andre for providing electron and field data from Cluster, G. Paschmann and J. Quinn for design of the EDI ambient mode, and T. Phan for many helpful discussions.

References

Bhattacharjee, A., K. Germaschewski, and C. S. Ng (2005), Current singularities: Drivers of impulsive reconnection, *Phys. Plasmas*, *12*, 042305, doi:10.1063/1.1872893.

Gustafsson, G., et al. (1997), The electric field and wave experiment for the Cluster mission, *Space Sci. Rev.*, *79*, 137.

Longmire, C. L. (1963), Elementary plasma physics, Wiley-Interscience, Hoboken, N. J.

Mozer, F. S., S. D. Bale, and T. D. Phan (2002), Evidence of diffusion regions at a sub-solar magnetopause crossing, *Phys. Rev. Lett.*, *89*, 015002, doi:10.1103/PhysRevLett.89.015002.

Mozer, F. S., et al. (2003), Observations of electron diffusion regions at the subsolar magnetopause, *Phys. Rev. Lett.*, *91*, 245002, doi:10.1103/PhysRevLett.91.245002.

Mozer, F. S. (2005), Criteria for and statistics of electron diffusion regions associated with sub-solar magnetic field reconnection, *J. Geophys. Res.*, doi:10.1029/2005JA011258, in press.

Paschmann, G., et al. (1997), The electron drift instrument for Cluster, *Space Sci. Rev.*, *79*, 233.

Russell, C. T., and R. C. Elphic (1979), ISEE observations of flux transfer events at the dayside magnetopause, *Geophys. Res. Lett.*, *6*, 33.

Shay, M. A., et al. (2001), Alfvenic collisionless magnetic reconnection and the Hall term, *J. Geophys. Res.*, *106*, 3759.

Vasyliunas, V. M. (1975), Theoretical models of magnetic field line merging, *Rev. Geophys.*, *13*, 303.

S. D. Bale, J. P. McFadden, and F. S. Mozer, Space Sciences Laboratory, University of California, Berkeley, Berkeley, CA 94720, USA. (fmozer@ssl.berkeley.edu)

R. B. Torbert, Physics Department, University of New Hampshire, Durham, NH 03824, USA.